Applied Surface Science 503 (2020) 144142

Contents lists available at ScienceDirect

Applied Surface Science

journal homepage: www.elsevier.com/locate/apsusc

Full Length Article

C_2H_2 semi-hydrogenation over the supported Pd and Cu catalysts: The effects of the support types, properties and metal-support interaction on C_2H_4 selectivity and activity

Zun Guan[a], Mifeng Xue[a], Zhiqin Li[b], Riguang Zhang[a,*], Baojun Wang[a]

[a] Key Laboratory of Coal Science and Technology of Ministry of Education and Shanxi Province, Taiyuan University of Technology, Taiyuan 030024, Shanxi, PR China
[b] College of Chemistry and Chemical Engineering, Xi'an Shiyou University, Xi'an 710065, Shaanxi, PR China

ARTICLE INFO

Keywords:
C_2H_2 semi-hydrogenation
Support
Metal-support interaction
Catalytic performance
Density functional theory

ABSTRACT

Aiming at identifying the effects of the support types, properties and the metal-support interaction of the supported catalysts on C_2H_4 selectivity and its formation activity for C_2H_2 semi-hydrogenation, the corresponding mechanism over the supported Pd and Cu catalysts with different supports are fully studied based on DFT calculations. This work indicates that the support types and properties change the selectivity of C_2H_4 and its formation activity, for the supported Pd catalysts, the oxygen-vacancy anatase and rutile TiO_2 supports present much better selectivity of C_2H_4 and its formation activity than the pure Pd catalyst does; especially, the anatase exhibits better catalytic performance than the rutile, in which the oxygen-vacancy show the crucial function. For the supported Cu catalysts, γ-Al_2O_3 is unable to enhance C_2H_4 selectivity compared to the pure Cu catalyst, whereas MgO support improves C_2H_4 selectivity but reduces its formation activity. Further, the metal-support interaction of the supported Pd catalysts are much stronger than that of the supported Cu catalyst, which results in better activity and selectivity of C_2H_4 over the supported Pd catalysts. This study can give out a valuable clue for the preparation of the supported Pd or Cu catalysts with better performance in C_2H_2 semi-hydrogenation.

1. Introduction

Removal of C_2H_2 from C_2H_4 feeds by the reaction of C_2H_2 semi-hydrogenating is thought to be crucial petrochemical processes [1–5]. The most commonly used catalyst in this reaction is the supported expensive metal Pd-based catalysts because of its high catalytic activity toward C_2H_4 formation [5–7]. Nevertheless, C_2H_2 and C_2H_4 are easy to be over-hydrogenated to ethane [1,8–10]. Thus, the metal promoters such as Au [11–13], Ag [8,14–16] or Cu [10,17–18] were added into the Pd catalyst to improve C_2H_4 selectivity. Nowadays, Cu-based catalysts also exhibited higher C_2H_4 selectivity in C_2H_2 semi-hydrogenation at a high temperature (> 473 K) [18–24]. For instance, Pd-doped Cu-based catalysts with the ratio of Cu: Pd of 50: 1 exhibits better selectivity of C_2H_4 and its formation activity in C_2H_2 semi-hydrogenation [21]. Kyriakou et al. [25] observed that the individual Pd atom doped into Cu(1 1 1) surface presents much better C_2H_4 selectivity than the pure Cu or Pd does.

The supported catalysts exhibit unusual catalytic properties and greatly affect heterogeneous catalytic reactions [26–28]. For instance, for the Pt NPs supported over the metal oxides with the strong metal-support interaction [29], in which the low-coordinated active centers of small Pt NPs exhibited better catalytic activity than the pure Pt for water-gas shift reaction and ethanol steam reforming reaction. In comparison with the unsupported Rh catalyst, the supported Rh/TiO_2 catalyst [30] promotes the formation of CH_3 species in syngas conversion instead of methanol. Further, the catalytic performance of the supported catalysts is closely related to the kinds of oxide support. Kattel et al. [29] investigated the mechanisms of CO_2 conversion by hydrogen over the supported Pd/TiO_2 and Pd/SiO_2 catalysts, indicating that TiO_2 support exhibits higher activity and selectivity toward CH_4 than SiO_2 support. Lalik et al [31] investigated the hydrogen and oxygen recombination reaction over the Pd-Au/SiO_2 and Pd-Au/Al_2O_3 catalysts, indicating that SiO_2 support exhibits higher catalytic activity and stability than Al_2O_3 support. Compared to Al_2O_3, SiO_2 and TiO_2 supports, MgO supported Fe-Co-Ni catalyst shows better catalytic performance for light olefins production in CO hydrogenation [32]. As for methane partial oxidation, Wang et al. [33] experimentally found that surface carbon was formed on Rh/SiO_2 catalyst; in contrast, no carbon deposition occurred on Rh/MgO catalyst, which is mainly determined by the high stability of Rh/MgO catalyst with the stronger metal-

* Corresponding author.
E-mail address: zhangriguang@tyut.edu.cn (R. Zhang).

https://doi.org/10.1016/j.apsusc.2019.144142
Received 20 July 2019; Received in revised form 19 September 2019; Accepted 20 September 2019
Available online 18 October 2019
0169-4332/

support interaction.

For the metal oxide support, the properties such as crystalline phase and oxygen vacancy also affect the catalytic performance. Firstly, for the crystalline phase, Al_2O_3 has different crystalline phases due to the different preparation methods, the physical and chemical properties of Al_2O_3 changed when the crystalline phase is different [34–37]. Komhom et al. [36] experimentally found the effect of mixed phase Al_2O_3 (α-, γ-, θ-) supported Pd catalysts with different α-phase content (0, 14, 47, 64, 100%) on C_2H_2 semi-hydrogenation, indicating that the proportion of α-phase reached 64%, C_2H_2 conversion and C_2H_4 selectivity increased significantly; the transition phase (γ-, θ-) accounted for about 36% increase the specific surface area, and improve the dispersion of Pd leading to good stability. Lambert et al. [37] experimentally indicated that Pd/γ-Al_2O_3 catalyst reached the highest C_2H_4 selectivity (85%) at 200℃ in C_2H_2 semi-hydrogenation, but C_2H_2 conversion was low (76%). For the TiO_2 support, Li et al. [38] found the strong metal-support interaction over the Pd catalyst supported by the anatase TiO_2, but not available for the Pd catalyst supported by the rutile TiO_2 at low temperature. Yang et al. [39] obtained higher selectivity of C_2H_4 and its formation activity for C_2H_2 semi-hydrogenation over the anatase TiO_2 supported Pd catalyst than that over the rutile TiO_2 support. On the other hand, for the oxygen-vacancy over the metal oxide supports, a large number of experimental studies suggested that the presence of oxygen-vacancy affects its catalytic performance by altering the metal-support interaction. As for CO oxidation, Wan et al. [40] prepared a single atomic site Au supported on the oxygen-vacancy TiO_2, and found that the oxygen-vacancy not only effectively stabilize Au atoms by forming the Ti-Au-Ti structure, but also promote the catalytic activity. Yang et al. [41] found that the interaction between the oxygen-vacancy anatase TiO_2(1 0 1) and Pd_4 cluster was much stronger than that between the perfect anatase TiO_2 and Pd_4 cluster, as a result, the oxygen-vacancy surface presents excellent activity for C_2H_2 semi-hydrogenation to form C_2H_4. Liu et al. [42] found that the metal-support interaction between Ni_4 and oxygen-vacancy MgO is much stronger than that between Ni_4 and perfect MgO, thus, the oxygen-vacancy Ni_4/MgO catalyst exhibits better activity toward CH_4 dissociation.

Yet, the mechanism of C_2H_2 semi-hydrogenation occurred over the metal oxides supported Pd and Cu catalysts are very limited so far, the effects of the support types, properties and metal-support interaction on the catalytic activity and selectivity of C_2H_2 semi-hydrogenation are still unclear. Thus, this work aims at elucidating the effects of the support types and properties on the selectivity of C_2H_4 and its formation activity, C_2H_2 semi-hydrogenation reactions over the supported Pd and Cu catalysts with different kinds of metal oxide supports were examined using density functional theory (DFT) calculations; then, the effect of metal-support interaction on the catalytic performance of the supported Pd and Cu catalysts toward C_2H_2 semi-hydrogenation is identified. The results are expected to provide some information about the support interaction for the experimental preparation of the supported catalysts with better-performance in C_2H_2 semi-hydrogenation.

2. Calculation methods and models

2.1. Calculation methods

In this study, all calculations are performed using Dmol^3 package [43,44], the GGA-PBE functional is used to describe exchange-correlation effects [45,46]. For the electron treatment, all electron is used for non-metal, while ECP [47] is used for metal atoms. A double-numerical basis with polarization functions (DNP) [48] is used for the valence electron functions. The complete LST/QST method [49,50] is performed to identify the transition states (TS). Meanwhile, TS confirmation together with frequency analysis is chosen to confirm the TS structure.

On the other hand, extensive researches [21,51,52] have demonstrated that the reaction conditions such as high temperature and high ratio of H_2/C_2H_2 can inhibit C_2H_2 polymerization to form green oil. Moreover, C_2H_2 semi-hydrogenation over Cu-based catalysts requires higher temperature [20,22]. Further, this study focuses on investigating the effects of the support types and properties on the activity and selectivity of the supported Pd and Cu catalysts in C_2H_2 semi-hydrogenation. Taking above analysis into consideration, the high H_2/C_2H_2 ratio and temperature are set to be 10 and 520 K is set to ignore the effect of C_2H_2 polymerization, and this work only examined C_2H_2 semi-hydrogenation on the supported Pd and Cu catalysts. Considering the realistic reaction conditions, H_2, C_2H_2 and C_2H_4 partial pressures are set to be 0.1, 0.01 and 0.89, respectively [23,24].

The adsorption free energies (G_{ads}) are defined using the following equation:

$$G_{ads} = E_{total} + G_{total} - (E_{adsorbate} + G_{adsorbate} + E_{catalyst} + G_{catalyst}) \quad (1)$$

where E_{total}, $E_{adsorbate}$ and $E_{catalyst}$ represent the energies of the system after adsorption, the adsorbent in the gas state and the supported catalyst, respectively. G_{total}, $G_{adsorbate}$ and $G_{catalyst}$ correspond to the Gibbs free energies at 520 K.

The interaction energies between the metal and the support, E_{int}, are calculated as follows:

$$E_{int} = E(\text{total}) - E(\text{metal}') - E(\text{support}') \quad (2)$$

where the E(metal′) denotes the total energy of Pd or Cu clusters supported on different supports, and the E(support′) represents the total energy of deformed support obtained after Pd or Cu cluster adsorption.

The activation free energy (ΔG_a) and reaction free energy (ΔG) are calculated on the basis of following equations:

$$\Delta G_a = (E_{TS} + G_{TS}) - (E_R + G_R) \quad (3)$$

$$\Delta G = (E_P + G_P) - (E_R + G_R) \quad (4)$$

where E_R, E_{TS}, and E_P correspond to the energies of reactants, transition states and products, respectively; the corresponding Gibbs free energies are represented by G_R, G_{TS} and G_P, respectively.

2.2. Computational models

In this study, the moderate size $Pd_{38}(Cu_{38})$ cluster is used as the active component of the supported catalysts, the outer shell Pd(Cu) atoms of $Pd_{38}(Cu_{38})$ cluster has 6 and 9 coordination numbers, which present the characteristics of (1 1 1) and (1 0 0) facets [53,54]; Moreover, previous research work [55,56] found that the effect of two layers atoms at the bottom of $Pd_{38}(Cu_{38})$ cluster on the adsorption and catalytic performance is not obvious. Thus, the half-part structure $Pd_{19}(Cu_{19})$ cluster is used to represent Pd(Cu) active component supported over the metal oxide. The $Pd_{19}(Cu_{19})$ cluster not only exhibits the structural characteristics of both $Pd_{38}(Cu_{38})$ cluster and Pd(1 1 1) (Cu(1 1 1)) surface, but also reduces the calculation time.

2.2.1. The supported Pd catalysts

For the supported Pd catalyst, four types of support widely used in C_2H_2 semi-hydrogenation, rutile TiO_2, anatase TiO_2, MgO and α-Al_2O_3, are considered. For the rutile and anatase TiO_2, previous studies [40,41] demonstrated that the presence of oxygen-oxygen significantly improve the metal-support interaction, which is favorable to enhance the stability and catalytic performance of the supported catalysts. Thus, the oxygen-vacancy rutile and anatase are used, which is denoted as TiO_2(1 1 0)-R-O_v and TiO_2(1 0 1)-A-O_v, respectively. TiO_2(1 1 0)-R-O_v surface is composed of a $p(4 \times 2)$ supercell with six-layers, the atoms in the bottom three layers are frozen. TiO_2(1 0 1)-A-O_v surface is composed of a twelve atomic layers $p(2 \times 3)$ suprtcell with four Ti atomic layers and eight O atomic layers), the uppermost six layers is relaxed during calculations. For the TiO_2 support, the oxygen-vacancy surface is formed by the removal of a bridge oxygen atom from the perfect TiO_2

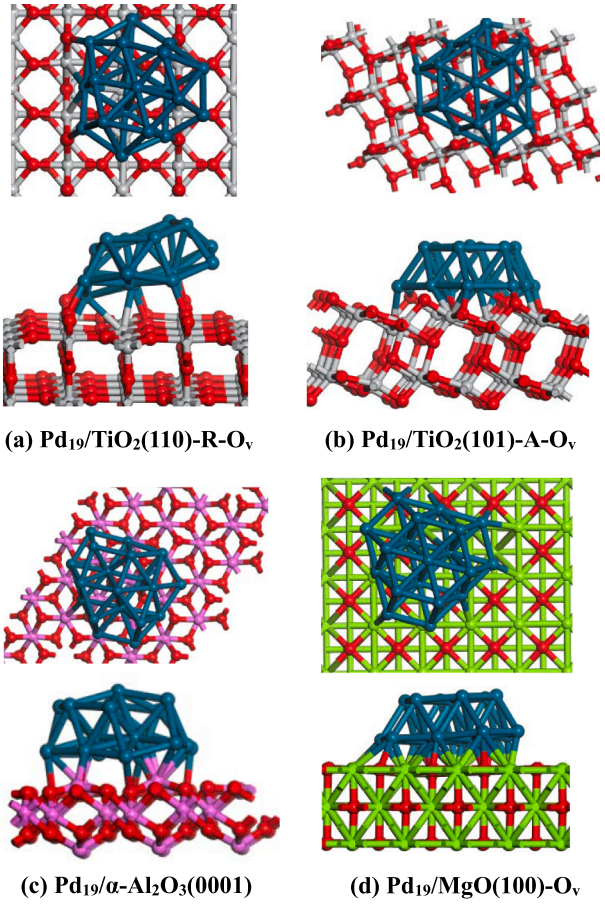

Fig. 1. Top view and side view of the supported Pd catalysts, (a) $Pd_{19}/TiO_2(1\,1\,0)$-R-O_v, (b) $Pd_{19}/TiO_2(1\,0\,1)$-A-O_v, (c) Pd_{19}/α-$Al_2O_3(0\,0\,0\,1)$ and (d) $Pd_{19}/MgO(1\,0\,0)$-O_v.

surface.

α-$Al_2O_3(0\,0\,0\,1)$ surface is composed of a four-layers $p(3 \times 3)$ supercell, the bottom one layer was frozen in the bulk positions. MgO (1 0 0) surface is composed of a $p(4 \times 5)$ supercell with three atomic layers, the oxygen-vacancy MgO surface is formed by the removal of one oxygen atom from the perfect surface; the bottom one layer is fixed.

For these metal oxide surfaces, the thickness of the vacuum layer is 12 Å. Fig. 1 shows the top-view and side-view of the supported Pd catalysts.

2.2.2. The supported Cu catalysts

For the supported Cu catalyst, two commonly used supports, γ-Al_2O_3 and MgO, are employed. For γ-Al_2O_3, the mainly exposed (1 0 0) is more easily dehydrated than the (1 1 0) surface [57]; C_2H_2 semi-hydrogenation on Cu-based catalysts operates at a higher temperature (> 460 K) [20,22], which is in favor of the formation of dehydrated surface; thus, the dehydrated γ-$Al_2O_3(1\,0\,0)$ surface is selected. γ-$Al_2O_3(1\,0\,0)$ surface is composed of an eight-layer $p(3 \times 2)$ supercell with the bottom three layers of atoms fixed. MgO (1 0 0) surface is consisted of a three-layer $p(4 \times 5)$ supercell, the bottom one layer is fixed, and the vacuum layer is 12 Å. The optimized structures of different supported Cu catalysts are shown in Fig. 2.

3. Results and discussion

3.1. Evaluation parameter of C_2H_4 selectivity

C_2H_4 feedstock contains a trace amount of C_2H_2 (< 1%) and large amount of C_2H_4 (> 89%). [52]. Therefore, only when C_2H_2 has

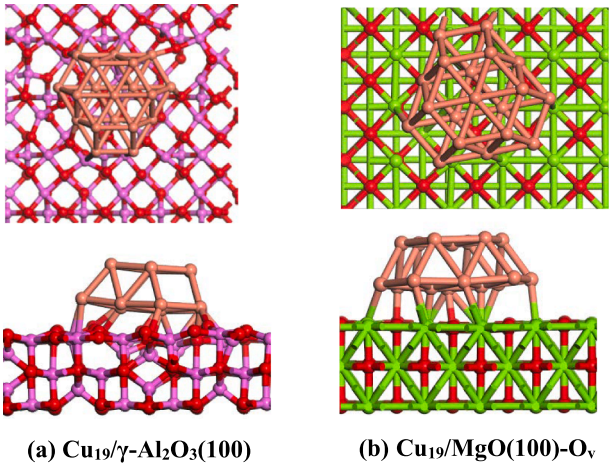

Fig. 2. Top view and side view of the supported Cu catalysts (a) Cu_{19}/γ-$Al_2O_3(1\,0\,0)$, (b)$Cu_{19}/MgO(1\,0\,0)$-O_v.

Table 1
Adsorption free energies of C_2H_x (x = 2–5) species over different supported Pd and Cu catalysts at 520 K.

Catalysts	Adsorption free energies (G_{ads}/kJ·mol^{-1})				
	C_2H_2	C_2H_3	C_2H_4	$CHCH_3$	C_2H_5
$Pd_{19}/TiO_2(1\,1\,0)$-R-O_v	−178.6	−195.0	−54.9	−308.1	−127.2
$Pd_{19}/TiO_2(1\,0\,1)$-A-O_v	−139.1	−229.5	−73.8	−312.2	−98.6
Pd_{19}/α-$Al_2O_3(0\,0\,0\,1)$	−201.0	−192.3	−63.6	−292.3	−97.8
$Pd_{19}/MgO(1\,0\,0)$-O_v	−178.8	−193.7	−57.1	−301.2	−136.8
Cu_{19}/γ-$Al_2O_3(1\,0\,0)$	−206.2	−253.0	−75.1	−359.5	−199.9
$Cu_{19}/MgO(1\,0\,0)$-O_v	−141.8	−244.4	−60.5	−325.9	−157.4

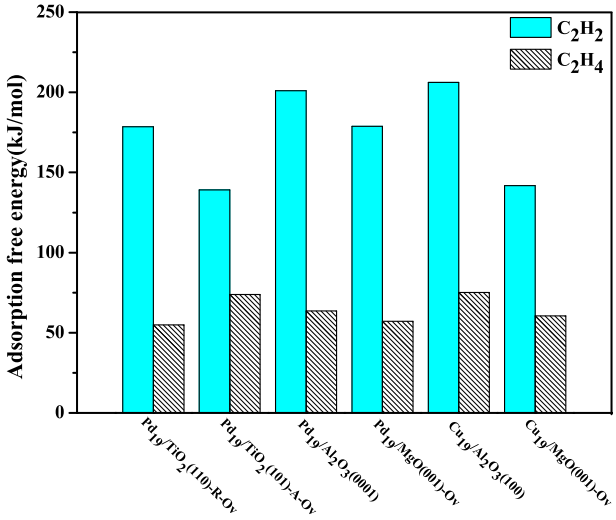

Fig. 3. The adsorption free energies of C_2H_2 and C_2H_4 over different supported Pd and Cu catalysts at 520 K.

stronger adsorption ability than C_2H_4, C_2H_2 impurities can be effectively removed from C_2H_4 feedstock. Consequently, the ability of C_2H_2 and C_2H_4 adsorption on the supported Pd and Cu catalysts are firstly considered (Table 1), Fig. 3 presents the adsorption free energies of C_2H_2 and C_2H_4, suggesting that C_2H_2 has stronger adsorption ability than C_2H_4 on all supported catalysts at 520 K, namely, a small quantities of C_2H_2 in large amount of C_2H_4 prefers to be adsorbed over the catalyst surface, which promotes C_2H_2 semi-hydrogenation.

For C_2H_2 semi-hydrogenation, a lot of the theoretical work only considered the effect of C_2H_4 intermediate route on C_2H_4 selectivity so

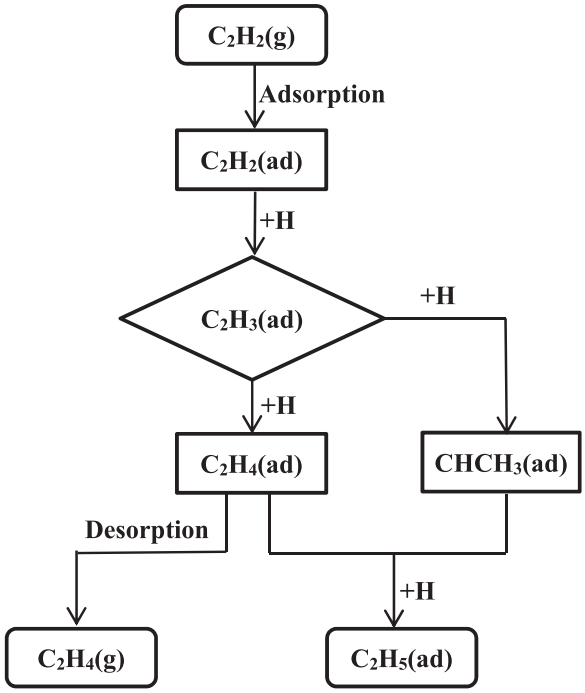

Fig. 4. The possible reaction routes of C_2H_2 semi-hydrogenation.

far [41,58–59]. For example, as Xu et al. [59] reported, the selectivity of C_2H_4 can be defined by calculating the energy difference between C_2H_4 hydrogenation and its desorption, but $CHCH_3$ intermediate route was not examined. As a matter of fact, the selectivity of C_2H_4 can be affected by $CHCH_3$ intermediate route. As a result, in our work, ***C_2H_4 desorption***, ***C_2H_4 intermediate*** and ***$CHCH_3$ intermediate*** routes of C_2H_2 semi-hydrogenation are investigated (see Fig. 4). Further, if the catalysts could promote C_2H_4 desorption route and inhibit the routes via C_2H_4 and $CHCH_3$ intermediates, the catalysts would be effective for the removal of C_2H_2 impurities.

This study firstly investigate the priority of C_2H_4 desorption and its hydrogenation, when C_2H_4 was easier to desorption rather than its hydrogenation to C_2H_5, the catalyst shows better selectivity of C_2H_4, which was defined as the energy difference by C_2H_4 hydrogenation barrier subtracting the absolute value of C_2H_4 adsorption energy, see the Eq. (5) [59]:

$$G_{sel} = \Delta G_a - |G_{ads}| \quad (5)$$

where ΔG_a and G_{ads} are C_2H_4 hydrogenation barrier and its adsorption energy, respectively.

On the other hand, when C_2H_4 desorption route was easier than its hydrogenation, the effect of $CHCH_3$ intermediate route on the selectivity of C_2H_4 needs to be further examined; moreover, when the overall barrier of $CHCH_3$ intermediate route is lower than that of C_2H_4 intermediate route, the value of C_2H_4 selectivity was defined as the overall free barrier difference between $CHCH_3$ intermediate and C_2H_4 desorption routes with respect to the C_2H_3 + H species, which was calculated using the Eq. (6):

$$G_{sel} = \Delta G_a(CHCH_3 \text{ intermediate}) - \Delta G_a(C_2H_4 \text{ desorption}) \quad (6)$$

where ΔG_a(CHCH$_3$ intermediate) and ΔG_a(C_2H_4 desorption) are the overall free barriers of $CHCH_3$ intermediate and C_2H_4 adsorption routes with respect to the C_2H_3 + H species, respectively. The more positive and larger values of G_{sel} means that the catalysts shows better selectivity of C_2H_4, namely, C_2H_4 desorption route prefers to occur instead of other two routes.

3.2. C_2H_2 semi-hydrogenation on the supported Pd catalysts

On the Pd_{19}/TiO_2(1 1 0)-R-O_v (Fig. 5(a)), C_2H_4 desorption is more preferred over its hydrogenation (54.9 *vs.* 107.4 kJ·mol^{-1}); meanwhile, starting from C_2H_3 + H species, C_2H_4 desorption route prefers to occur in kinetics instead of $CHCH_3$ intermediate route (104.1 *vs.* 155.4 kJ·mol^{-1}); thus, the gaseous C_2H_4 is dominant product with the corresponding selectivity value G_{sel} of 52.5 kJ·mol^{-1}. Similarly, on the Pd_{19}/TiO_2(1 0 1)-A-O_v (Fig. 5(b)), C_2H_4 desorption route to form gas phase C_2H_4 is still dominant with the selectivity value of 127.8 kJ·mol^{-1}.

For the Pd_{19}/α-Al_2O_3(0 0 0 1) (Fig. 5(c)), C_2H_4 desorption is much easier in kinetics than its hydrogenation (63.6 *vs.* 184.6 kJ·mol^{-1}), however, $CHCH_3$ intermediate route to form ethane is more favorable in kinetics than C_2H_4 desorption route (248.9 *vs.* 288.9 kJ·mol^{-1}), suggesting that the Pd_{19}/α-Al_2O_3(0 0 0 1) catalyst exhibits low selectivity of C_2H_4 (−40.0 kJ·mol^{-1}). For the Pd_{19}/MgO(1 0 0)-O_v (Fig. 5(d)), C_2H_4 desorption route is preferred in kinetics over its hydrogenation (57.1 *vs.* 213.5 kJ·mol^{-1}), however, the overall free barrier of $CHCH_3$ intermediate route is higher by 9.5 kJ·mol^{-1} than that of C_2H_4 desorption route (257.3 *vs.* 247.8 kJ·mol^{-1}), thus, C_2H_4 desorption route is competitive with $CHCH_3$ intermediate route, the catalyst exhibits weak selectivity of C_2H_4 (9.5 kJ·mol^{-1}).

For the unsupported Pd_{38} cluster (Fig. S2), C_2H_4 over-hydrogenation to ethane easily occur with the selectivity value G_{sel} of −73.1 kJ·mol^{-1}, namely, the unsupported Pd_{38} cluster exhibits very poor C_2H_4 selectivity.

In general, in comparison with the unsupported Pd_{38} cluster, the support of the supported Pd catalysts obviously improve the selectivity of C_2H_4 (−73.1 *vs.* 52.5, 127.8, −40.0 and 9.5 kJ·mol^{-1}) over the Pd_{19}/TiO_2(1 1 0)-R-O_v, Pd_{19}/TiO_2(1 0 1)-A-O_v, Pd_{19}/α-Al_2O_3(0 0 0 1) and Pd_{19}/MgO(1 0 0)-O_v catalysts, which depend on the types of the used support. Especially, the anatase and rutile TiO_2 supports thoroughly improve the selectivity of C_2H_4 (127.8 and 52.5 kJ·mol^{-1}), whereas the α-Al_2O_3 and MgO supports still lead to the formation of ethane due to the occurrence of $CHCH_3$ intermediate route with poor C_2H_4 selectivity.

3.3. C_2H_2 semi-hydrogenation on the supported Cu catalysts

On the Cu_{19}/γ-Al_2O_3(1 0 0) (Fig. 6(a)), C_2H_4 desorption is more preferred in kinetics over its hydrogenation (75.1 *vs.* 182.9 kJ·mol^{-1}). However, starting from the C_2H_3 + H species, $CHCH_3$ intermediate route is much preferred in kinetics over C_2H_4 desorption route (68.4 *vs.* 111.8 kJ·mol^{-1}). Thus, $CHCH_3$ intermediate route to form ethane becomes dominant, which corresponds to the selectivity value G_{sel} of −43.4 kJ·mol^{-1}. For the Cu_{19}/MgO(1 0 0)-O_v (Fig. 6(b)), C_2H_4 desorption route becomes dominant corresponding to the selectivity value G_{sel} of 101.3 kJ·mol^{-1}. Further, for the unsupported Cu_{38} cluster (Fig. S3), C_2H_4 hydrogenation to C_2H_5 is superior to C_2H_4 desorption in kinetics (73.7 *vs.* 95.6 kJ·mol^{-1}), suggesting that the unsupported Cu_{38} cluster is easily over-hydrogenated to form ethane, and exhibits poor selectivity of C_2H_4 (−21.9 kJ·mol^{-1}).

As mentioned above, in comparison with the unsupported Cu_{38} cluster, γ-Al_2O_3 support decreased C_2H_4 selectivity (−43.4 *vs.* −21.9 kJ·mol^{-1}), whereas the oxygen-vacancy MgO support significantly improve C_2H_4 selectivity (101.3 *vs.* −21.9 kJ·mol^{-1}). Thus, the types of support also affect C_2H_4 selectivity over the supported Cu catalysts.

3.4. General discussion

Based on above analysis, the supported Pd and Cu catalysts with better selectivity of C_2H_4 have been obtained, subsequently, the formation activity of C_2H_4 is described by calculating the rate of C_2H_2 semi-hydrogenation to C_2H_4, in which the proposed two-step model in

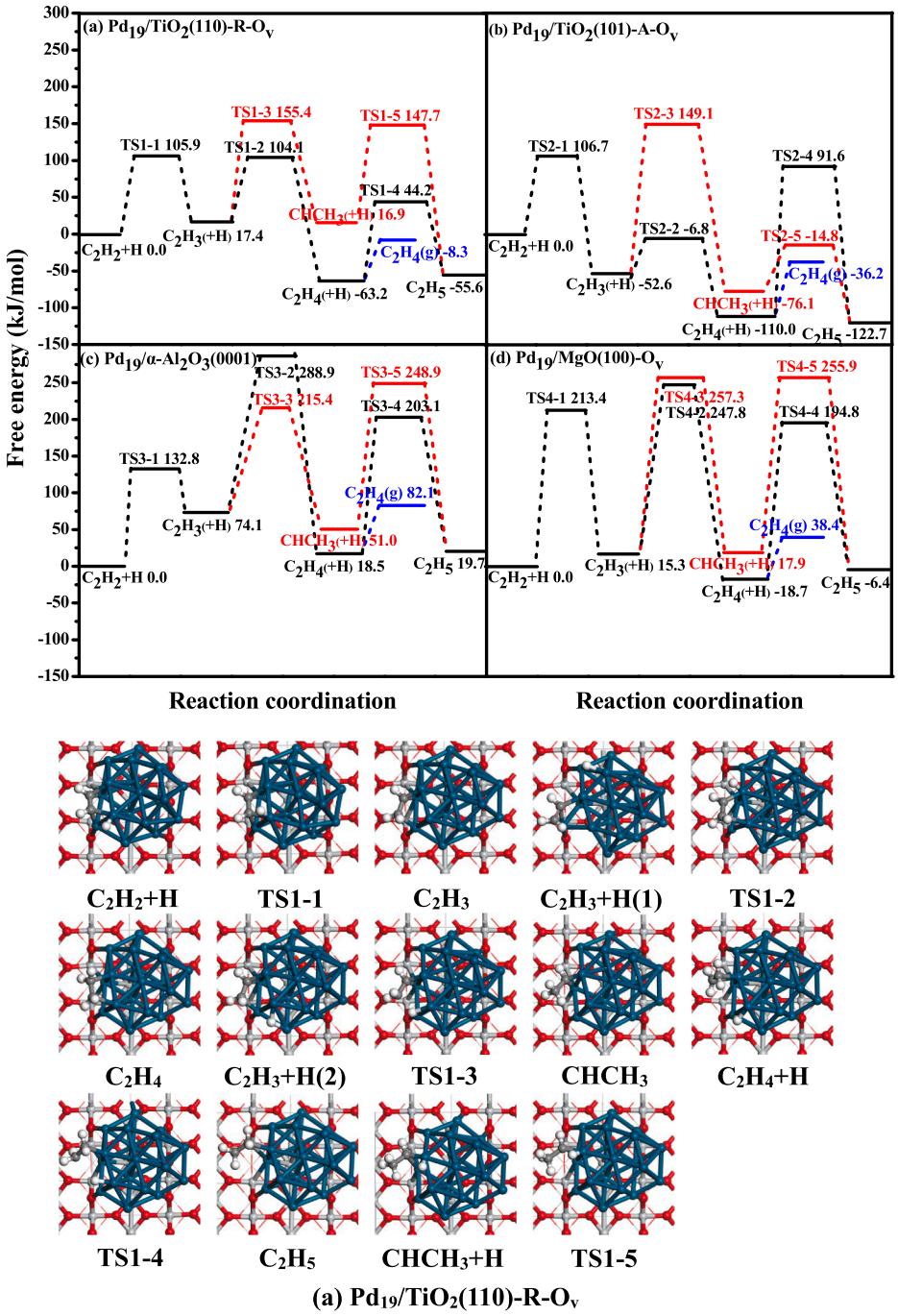

Fig. 5. Free energy profiles of three routes involving in C_2H_2 semi-hydrogenation on the supported Pd catalysts. (a) Pd_{19}/TiO_2(1 1 0)-R-O_v, (b) Pd_{19}/TiO_2(1 0 1)-A-O_v, (c) Pd_{19}/α-Al_2O_3(0 0 0 1) and (d) Pd_{19}/MgO(1 0 0)-O_v together with the structures of ISs, TSs and FSs.

the studies of Hu et al. [60–62] is employed (see details in the Supplementary Material). Table 2 lists the rates of C_2H_4 formation over the supported Pd and Cu catalysts with better C_2H_4 selectivity.

3.4.1. Effects of support types and properties on the selectivity and activity

For the supported Pd catalysts (see Fig. 7 and Table 2), the selectivity of C_2H_4 formation (G_{sel}/kJ·mol^{-1}) over the supported Pd catalysts follows the order: $Pd_{38}(-73.1)$ < Pd_{19}/α-Al_2O_3(0 0 0 1)(−40.0) < Pd_{19}/MgO(1 0 0)-O_v(9.5) < Pd_{19}/TiO_2(1 1 0)-R-O_v(52.5) < Pd_{19}/TiO_2(1 0 1)-A-O_v(127.8); The rate (r/s^{-1}·site^{-1}) corresponding to C_2H_4 formation follows the order: Pd_{19}/MgO(1 0 0)-O_v(4.03×10^{-12}) < Pd_{38}(8.71×10^{-2}) < Pd_{19}/TiO_2(1 1 0)-R-O_v(6.16×10^{0}) < Pd_{19}/TiO_2(1 0 1)-A-O_v(6.19×10^{5}). Thus, compared to the unsupported Pd catalyst, the supports of α-Al_2O_3 and oxygen-vacancy MgO still show poor C_2H_4 selectivity and lower C_2H_4 formation activity, whereas the oxygen-vacancy anatase and rutile TiO_2 supports exhibit higher selectivity of C_2H_4 and its formation activity.

For the supported Cu catalysts (see Fig. 7 and Table 2), the selectivity of C_2H_4 follows the order: Cu_{19}/γ-Al_2O_3(1 0 0) (−43.4) < Cu_{38}(−21.9) < Cu_{19}/MgO(1 0 0)-O_v(101.3); and the sequence of reaction rate (r/s^{-1}·site^{-1}) is: Cu_{19}/MgO(1 0 0)-O_v(6.87×10^{-5}) < Cu_{38}(1.79×10^{-3}).

As mentioned above, the selectivity of C_2H_4 and its formation activity in C_2H_2 semi-hydrogenation on the supported Cu and Pd catalysts depend on the types of the support. Meanwhile, the supported Pd catalyst is more favorable to improve the selectivity of C_2H_4 than the supported Cu catalyst, namely, the newly-efficient Pd-based catalysts

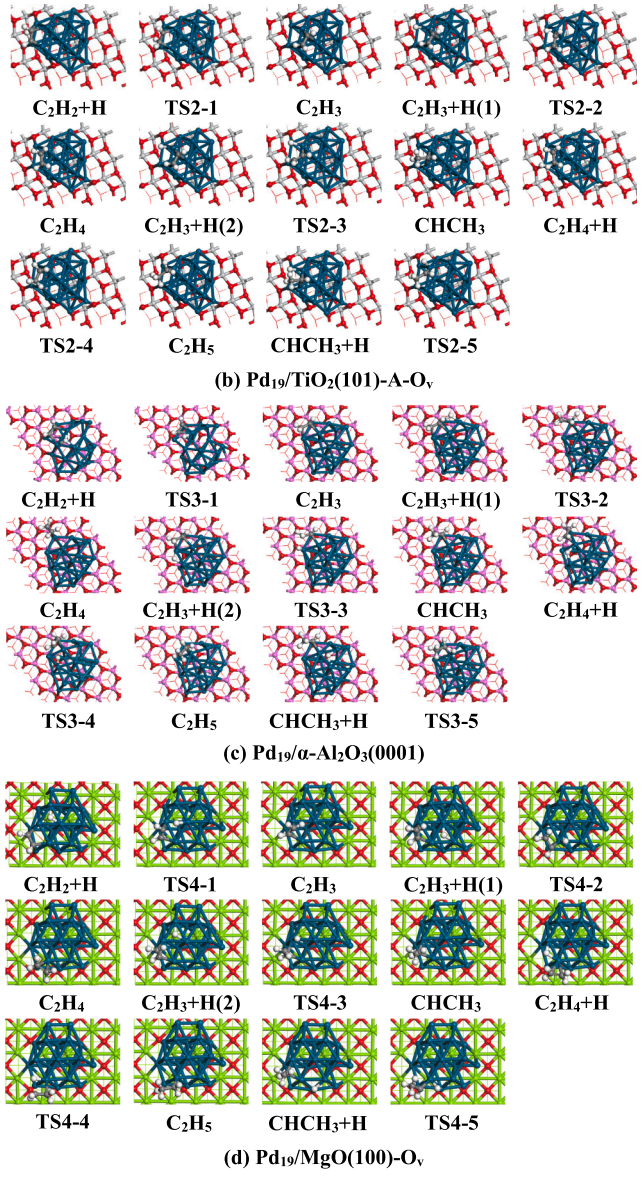

Fig. 5. (*continued*)

should focus on the supported Pd-based catalyst instead of the supported Cu-based catalysts. Further, the oxygen-vacancy anatase TiO_2 support exhibits higher selectivity of C_2H_4 and its formation activity than the oxygen-vacancy rutile TiO_2. Experimental observations by Kontapakdee et al. [63] also found that the Pd/TiO_2-anatase exhibited higher C_2H_2 conversion and C_2H_4 selectivity than the rutile TiO_2 supported ones, and the oxygen-vacancy surface has better activity for C_2H_2 semi-hydrogenation than the perfect surface. Thus, the support properties such as the crystalline phase and surface oxygen-vacancy affect the catalytic performance of the supported catalysts.

3.4.2. Effects of metal-support interaction on the selectivity and activity

In order to clarify the effects of support types and properties on the catalytic activity and selectivity in C_2H_2 semi-hydrogenation, the interaction and charge distribution between the metal composition and the support were further calculated for the supported Pd and Cu catalysts.

As shown in Table 3, the interaction energies (kJ·mol^{-1}) between Pd_{19} cluster and different supports follows the order: Pd_{19}/TiO_2(1 1 0)-R-O_v(−670.0) < Pd_{19}/α-Al_2O_3(0 0 0 1)(−768.5) < Pd_{19}/MgO (1 0 0)-O_v(−901.8) < Pd_{19}/TiO_2(1 0 1)-A-O_v(−1007.4), the metal-support interaction between Pd_{19} cluster and the oxygen-vacancy anatase TiO_2 support is much stronger than that the other supported Pd catalysts, thus, Pd_{19}/TiO_2(1 0 1)-A-O_v catalyst presents higher C_2H_4 selectivity and its formation activity. Moreover the average charge of Pd atom on Pd_{19}/TiO_2(1 0 1)-A-O_v catalyst is −0.159 *e*, which is more negative than those (−0.154 *e*, −0.149 *e* and −0.150 *e*) on the other supported Pd catalysts, suggesting that for the supported Pd catalyst, the stronger metal-support interaction can enhance the selectivity of C_2H_4 and its formation activity.

For the supported Cu catalysts, the interaction energies (kJ·mol^{-1}) between Cu_{19} cluster and different supports follows the order of Cu_{19}/γ-Al_2O_3(−695.5) < Cu_{19}/MgO(1 0 0)-O_v(−725.3), the average charge of Cu atom on Cu_{19}/MgO(1 0 0)-O_v catalyst is also more negative than that on Cu_{19}/γ-Al_2O_3 catalyst (−0.240 *e vs.* −0.095 *e*), as a result, Cu_{19}/MgO(1 0 0)-O_v catalyst exhibits higher C_2H_4 selectivity and its formation activity than Cu_{19}/γ-Al_2O_3 catalyst.

In general, the stronger metal-support interaction in the supported Pd and Cu catalysts is in favor of enhancing the selectivity of C_2H_4 and its formation activity. Moreover, the interaction between the support and Pd is much stronger than that between the support and Cu. Thus, in comparison with the supported Cu catalyst, the supported Pd catalyst, especially Pd_{19}/TiO_2(1 0 1)-A-O_v, is the best candidate catalyst in C_2H_2 semi-hydrogenation.

3.4.3. The analysis of electronic structure

As mentioned above, the supported Pd catalyst is more suitable to form gaseous C_2H_4 in C_2H_2 semi-hydrogenation, the local density of states (*p*DOS) for the Pd atom of the supported Pd catalysts were calculated. As shown in Fig. 8(a–c), *d*-band center of different supported Pd catalysts follows the sequence of Pd_{19}/TiO_2(1 0 1)-A-O_v(−2.55) < Pd_{19}/TiO_2(1 1 0)−R-O_v(−1.81) < Pd_{19}/MgO(1 0 0)-O_v(−1.55). Among them, the *d*-band center for the Pd atoms of Pd_{19}/TiO_2(1 0 1)-A-O_v and Pd_{19}/TiO_2(1 1 0)-R-O_v catalysts tends to stay away from the Fermi level than that of Pd_{19}/MgO(1 0 0)-O_v catalyst, especially, Pd_{19}/TiO_2(1 0 1)-A-O_v. Thus, for the supported Pd catalysts, the support types and properties alter the *d*-orbital distribution of active component metal, and therefore affect the adsorption and activation process of the species on the catalysts, and further regulate the selectivity of C_2H_4 and its formation activity for C_2H_2 semi-hydrogenation. The oxygen-vacancy anatase TiO_2 support increase the distance between the *d*-band center of active Pd atom and the Fermi level, resulting in the highest activity.

4. Conclusions

This work aims at identifying the functions of the support types, properties and metal-support interaction in affecting the selectivity of C_2H_4 and its formation activity for C_2H_2 semi-hydrogenation; different supported Pd and Cu catalysts are examined. The results show that the support types affect the selectivity of C_2H_4 and its formation activity; for the supported Pd catalysts, both α-Al_2O_3 and oxygen-vacancy MgO supports present low C_2H_4 selectivity and its formation activity, while the oxygen-vacancy anatase and rutile TiO_2 supports show better selectivity of C_2H_4 and its formation activity. For the supported Cu catalysts, γ-Al_2O_3 support shows lower C_2H_4 selectivity in contrast to the unsupported Cu catalyst, whereas the oxygen-vacancy MgO support effectively enhances the selectivity of C_2H_4 but reduced its formation activity. On the other hand, the support properties such as crystalline phase and oxygen-vacancy affect the selectivity of C_2H_4 and its formation activity; the anatase TiO_2 support exhibits better catalytic

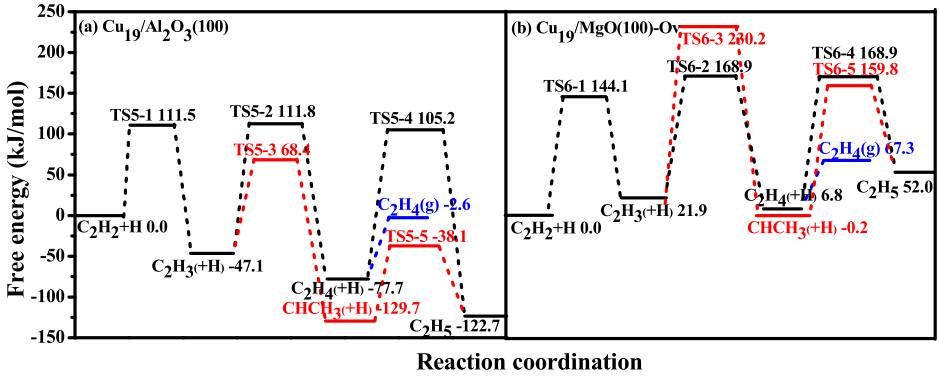

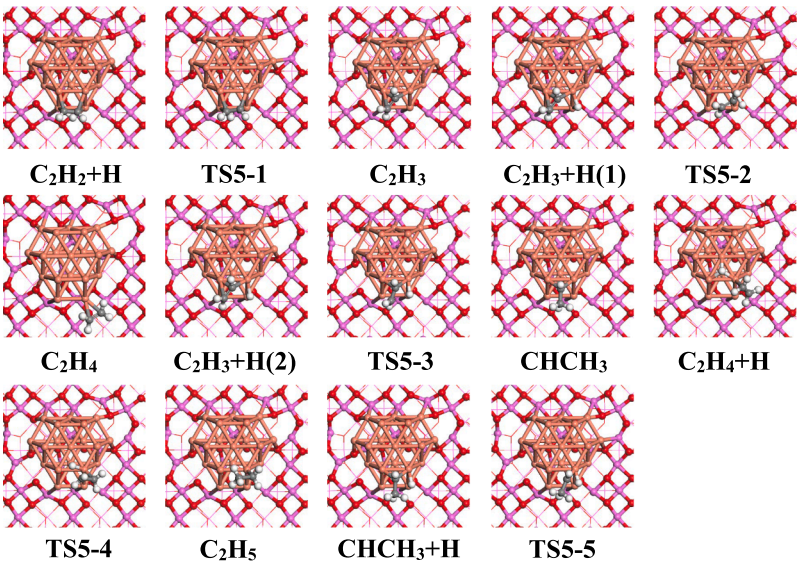

(a) $Cu_{19}/\gamma\text{-}Al_2O_3(100)$

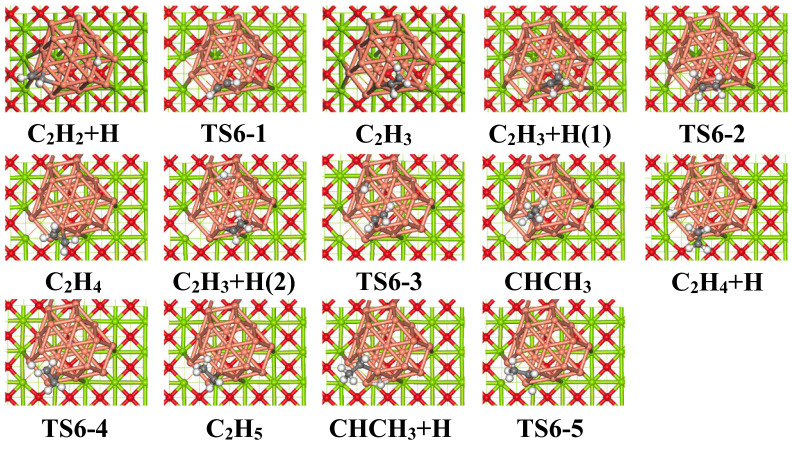

(b) $Cu_{19}/MgO(100)\text{-}O_v$

Fig. 6. Free energy profiles of three routes involving in C_2H_2 semi-hydrogenation on (a) $Cu_{19}/\gamma\text{-}Al_2O_3(1\,0\,0)$ and (b) $Cu_{19}/MgO(1\,0\,0)\text{-}O_v$ together with the structures of ISs, TSs and FSs.

Table 2
The values of $G_R^{ad} - G_R^{de} + G_P^{de}$, G_P^{de}(kJ·mol^{-1}), the reaction rate (r/s^{-1}·site^{-1}) and the selectivity (G_{sel}/kJ·mol^{-1}) of C_2H_4 formation at 520 K over different supported Pd and Cu catalysts, as well as the unsupported Pd and Cu clusters.

Clusters	G_{sel}	r
Pd_{19}/TiO_2(1 1 0)-R-O_v	52.5	6.16×10^{0}
Pd_{19}/TiO_2(1 0 1)-A-O_v	127.8	6.19×10^{5}
Pd_{19}/α-Al_2O_3(0 0 0 1)	−40.0	/
Pd_{19}/MgO(1 0 0)-O_v	9.5	4.03×10^{-12}
Cu_{19}/γ-Al_2O_3(1 0 0)	−43.4	/
Cu_{19}/MgO(1 0 0)-O_v	101.3	6.87×10^{-5}
Pd_{38}	−73.1	8.71×10^{-2}
Cu_{38}	−21.9	1.79×10^{-3}

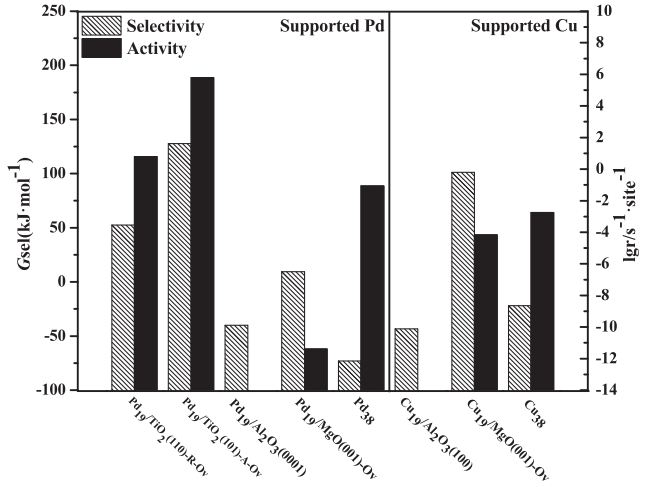

Fig. 7. The selectivity (G_{sel}/kJ·mol^{-1}) and activity (lgr/s^{-1}·site^{-1}) of C_2H_4 formation in C_2H_2 semi-hydrogenation over the supported Pd and Cu catalysts.

Table 3
The interaction energies (E_{int}/kJ·mol^{-1}) between the metal and the support for the supported Pd and Cu catalysts together with the Mulliken charges of Pd(Cu) atoms (e).

Catalysts	E_{int} (kJ·mol^{-1})	Pd/Cu charge
Pd_{19}/TiO_2(1 1 0)-R-O_v	−670.0	−0.154
Pd_{19}/TiO_2(1 0 1)-A-O_v	−1007.4	−0.159
Pd_{19}/α-Al_2O_3(0 0 0 1)	−768.5	−0.149
Pd_{19}/MgO(1 0 0)-O_v	−901.8	−0.150
Cu_{19}/γ-Al_2O_3(1 0 0)	−695.5	−0.095
Cu_{19}/MgO(1 0 0)-O_v	−725.3	−0.240

performance toward C_2H_4 formation than the rutile phase, moreover, the surface oxygen-vacancy significantly enhance the selectivity of C_2H_4 and its formation activity. Further, the supported Pd catalysts exhibit better catalytic performance than the supported Cu catalysts, which is attributed to that the metal-support interaction of the supported Pd catalysts was much stronger than that of the supported Cu catalysts. Thus, the supported Pd catalyst, especially Pd_{19}/TiO_2(1 0 1)-A-O_v catalyst, is the promising catalyst for C_2H_2 semi- hydrogenation.

Declaration of Competing Interest

The authors declare that they have no known competing financial interests or personal relationships that could have appeared to influence the work reported in this paper.

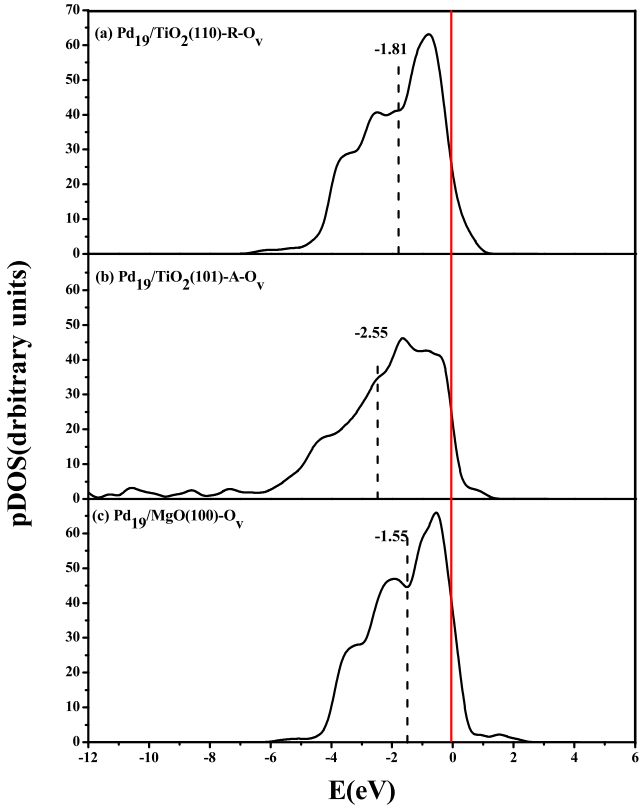

Fig. 8. Projected density of states (*p*DOS) plots of the *d*-orbitals for the supported Pd and Cu catalysts. (a) Pd_{19}/TiO_2(1 1 0)-R-O_v, (b) Pd_{19}/TiO_2(1 0 1)-A-O_v and (c) Pd_{19}/MgO(1 0 0)-O_v.

Acknowledgment

This work is financially supported by the National Natural Science Foundation of China (No. 21776193), the Key projects of National Natural Science Foundation of China (No. 21736007) and the Top Young Innovative Talents of Shanxi, and U.S. NSF-sponsored NCAR-Wyoming Supercomputing Center (NWSC).

Appendix A. Supplementary material

The detailed descriptions about all the stable adsorption configuration of C_2H_x(x = 2–5) species, the structures of initial states, transition states, final states involving in C_2H_2 semi-hydrogenation over different supported Pd and Cu catalysts, as well as two-step model of C_2H_4 formation have been presented. Supplementary data to this article can be found online at https://doi.org/10.1016/j.apsusc.2019.144142.

References

[1] P.A. Sheth, M. Neurock, C.M. Smith, A first-principles analysis of acetylene hydrogenation over Pd(111), J. Phys. Chem. B 107 (2003) 2009–2017.
[2] Q.W. Zhang, J. Li, X.X. Liu, Q.M. Zhu, Synergetic effect of Pd and Ag dispersed on Al_2O_3 in the selective hydrogenation of acetylene, Appl. Catal. A: Gen. 197 (2000) 221–228.
[3] F.M. McKenna, J.A. Anderson, Selectivity enhancement in acetylene hydrogenation over diphenyl sulphide-modified Pd/TiO_2 catalysts, J. Catal. 281 (2011) 231–240.
[4] Suthana Chinayon, Okorn Mekasuwandumrong, Piyasan Praserthdam, Joongjai Panpranot, Selective hydrogenation of acetylene over Pd catalysts supported on nanocrystalline α-Al_2O_3 and Zn-modified α-Al_2O_3, Catal. Commun. 9 (14) (2008) 2297–2302, https://doi.org/10.1016/j.catcom.2008.03.032.
[5] J.H. Kang, E.W. Shin, W.J. Kim, J.D. Park, S.H. Moon, Selective hydrogenation of acetylene on TiO_2-added Pd catalysts, J. Catal. 208 (2002) 310–320.
[6] J.H. Kang, E.W. Shin, W.J. Kim, J.D. Park, S.H. Moon, Selective hydrogenation of acetylene on Pd/SiO_2 catalysts promoted with Ti, Nb and Ce oxides, Catal. Today 63 (2000) 183–188.
[7] Y.Y. Zhang, W.J. Diao, C.T. Williams, J.R. Monnier, Selective hydrogenation of

acetylene in excess ethylene using Ag- and Au–Pd/SiO_2 bimetallic catalysts prepared by electroless deposition, Appl. Catal. A: Gen. 469 (2014) 419–426.
[8] B. Ngamsom, N. Bogdanchikova, M.A. Borja, P. Praserthdam, Characterisations of Pd–Ag/Al_2O_3 catalysts for selective acetylene hydrogenation: effect of pretreatment with NO and N_2O, Catal. Commun. 5 (2004) 243–248.
[9] J. Osswald, K. Kovnir, M. Armbrüster, R. Giedigkeit, R.E. Jentoft, U. Wild, Y. Grin, R. Schlögl, Palladium–gallium intermetallic compounds for the selective hydrogenation of acetylene: Part II: surface characterization and catalytic performance, J. Catal. 258 (2008) 219–227.
[10] S.K. Kim, J.H. Lee, I.Y. Ahn, W.J. Kim, S.H. Moon, Performance of Cu-promoted Pd catalysts prepared by adding Cu using a surface redox method in acetylene hydrogenation, Appl. Catal. A: Gen. 401 (2011) 12–19.
[11] A. Sárkány, O. Geszti, G. Sáfrán, Preparation of Pd_{shell}–Au_{core}/SiO_2 catalyst and catalytic activity for acetylene hydrogenation, Appl. Catal. A: Gen. 350 (2008) 157–163.
[12] T.V. Choudhary, C. Sivadinarayana, A.K. Datye, D. Kumar, D.W. Goodman, Acetylene hydrogenation on Au-based catalysts, Catal. Lett. 86 (2003) 1–8.
[13] A. Sárkány, A. Horváth, A. Beck, Hydrogenation of acetylene over low loaded Pd and Pd-Au/SiO_2 catalysts, Appl. Catal. A: Gen. 229 (2015) 117–125.
[14] G.X. Pei, X.Y. Liu, A. Wang, A.F. Lee, M.A. Isaacs, L. Li, X. Pan, X. Yang, X. Wang, Z. Tai, Ag alloyed Pd single-atom catalysts for efficient selective hydrogenation of acetylene to ethylene in excess ethylene, ACS Catal. 5 (2015) 3717–3725.
[15] N.A. Khan, S. Shaikhutdinov, H.J. Freund, Acetylene and ethylene hydrogenation on alumina supported Pd-Ag model catalysts, Catal. Lett. 108 (2006) 159–164.
[16] J.H. Lee, S.K. Kim, I.Y. Ahn, W.J. Kim, S.H. Moon, Performance of Pd–Ag/Al_2O_3 catalysts prepared by the selective deposition of Ag onto Pd in acetylene hydrogenation, Catal. Commun. 12 (2011) 1251–1254.
[17] L. Guczi, Z. Schay, G. Stefler, L.F. Liotta, G. Deganello, A.M. Venezia, Pumice-supported Cu-Pd catalysts: influence of copper on the activity and selectivity of palladium in the hydrogenation of phenylacetylene and but-1-ene, J. Catal. 182 (1999) 456–462.
[18] S. Leviness, V. Nair, A.H. Weiss, Z. Schay, L. Guczi, Acetylene hydrogenation selectivity control on PdCu/Al_2O_3 catalysts, J. Mol. Catal. 25 (1984) 131–140.
[19] J.T. Wehrli, D.J. Thomas, M.S. Wainwright, D.L. Trimm, N.W. Cant, Selective hydrogenation of propyne over supported copper catalysts: influence of support, Appl. Catal. 70 (1991) 253–262.
[20] M.R. Stammbach, D.J. Thomas, D.L. Trimm, M.S. Wainwright, Hydrogenation of ethyne over an ion-exchanged copper on silica catalyst, Appl. Catal. 58 (1990) 209–217.
[21] A.J. McCue, C.J. McRitchie, A.M. Shepherd, J.A. Anderson, Cu/Al_2O_3 catalysts modified with Pd for selective acetylene hydrogenation, J. Catal. 319 (2014) 127–135.
[22] B. Bridier, M.A.G. Hevia, N. López, J. Pérez-Ramírez, Permanent alkene selectivity enhancement in copper-catalyzed propyne hydrogenation by eemporary CO supply, J. Catal. 278 (2011) 167–172.
[23] R.G. Zhang, B. Zhao, L.L. He, A.J. Wang, B.J. Wang, Cost-effective promoter-doped Cu-based bimetallic catalysts for the selective hydrogenation of C_2H_2 to C_2H_4: the effect of the promoter on selectivity and activity, Phys. Chem. Chem. Phys. 20 (2018) 17487–17496.
[24] R.G. Zhang, B. Zhao, L.X. Ling, A.J. Wang, C.K. Russell, B.J. Wang, M.H. Fan, A cost-effective Pd-doped Cu bimetallic materials to tuning selectivity and activity using doped atom ensembles as active sites for efficient removal of acetylene from ethylene, Chem. Cat. Chem. 10 (2018) 2424–2432.
[25] G. Kyriakou, M.B. Boucher, A.D. Jewell, E.A. Lewis, T.J. Lawton, A.E. Baber, H.L. Tierney, M.F. Stephanopoulos, E.C.H. Sykes, Isolated metal atom geometries as a strategy for selective heterogeneous hydrogenations, Science 335 (2012) 1209–1212.
[26] H. Yoshida, T. Nakajima, Y. Yazawa, T. Hattori, Support effect on methane combustion over palladium catalysts, Appl. Catal. B: Environ. 71 (2007) 70–79.
[27] P. Sangeetha, K. Shanthi, K.S. RamaRao, B. Viswanathan, P. Selvam, Hydrogenation of nitrobenzene over palladium-supported catalysts—effect of support, Appl. Catal. A: Gen. 353 (2009) 160–165.
[28] T. Nanba, S. Masukawa, J. Uchisawa, A. Obuchi, Effect of support materials on Ag catalysts used for acrylonitrile decomposition, J. Catal. 259 (2008) 250–259.
[29] S. Kattel, B.H. Yan, J.G. Chen, P. Liu, CO_2 hydrogenation on Pt, Pt/SiO_2 and Pt/TiO_2: importance of synergy between Pt and oxide support, J. Catal. 343 (2016) 115–126.
[30] R.G. Zhang, M. Peng, B.J. Wang, Catalytic selectivity of Rh/TiO_2 catalyst in syngas conversion to ethanol: probing into the mechanism and functions of TiO_2 support and promoter, Catal. Sci. Technol. 7 (2017) 1073–1085.
[31] E. Lalik, A. Drelinkiewicz, R. Kosydar, R. Tokarz-Sobieraj, M. Witko, T. Szumełda, J. Gurgul, D. Duraczynska, A role of Au-content in performance of Pd-Au/SiO_2 and Pd-Au/Al_2O_3 catalyst in the hydrogen and oxygen recombination reaction. The microcalorimetric and DFT studies, Appl. Catal. A: Gen. 517 (2016) 196–210.
[32] A.A. Mirzaei, S. Vahid, H.O. Torshizi, Effect of support and promoter on the catalytic performance and structural properties of the Fe-Co-Ni catalysts for CO hydrogenation, J. Nat. Gas. Sci. Eng. 15 (2013) 106–117.
[33] H.Y. Wang, E. Ruckenstein, Partial oxidation of methane to synthesis gas over MgO- and SiO_2-supported rhodium catalysts, J. Catal. 186 (1999) 181–187.
[34] S. Komeili, M.T. Ravanchi, A. Taeb, The influence of alumina phases on the performance of the Pd-Ag/Al_2O_3 catalyst in tail-end selective hydrogenation of acetylene, Appl. Catal. A: Gen. 502 (2015) 287–296.
[35] S. Chinayon, O. Mekasuwandumrong, P. Praserthdam, J. Panpranot, Selective hydrogenation of acetylene over Pd catalysts supported on nanocrystalline α-Al_2O_3 and Zn-modified α-Al_2O_3, Catal. Commun. 9 (2008) 2297–2302.
[36] S. Komhom, O. Mekasuwandumrong, P. Praserthdam, J. Panpranot, Improvement of Pd/Al_2O_3 catalyst performance in selective acetylene hydrogenation using mixed phases Al_2O_3 support, Catal. Commun. 10 (2008) 86–91.
[37] C.K. Lambert, R.D. Gonzalez, Activity and selectivity of a Pd/γ-Al_2O_3 catalytic membrane in the partial hydrogenation reactions of acetylene and 1,3-butadiene, Catal. Lett. 57 (1999) 1–7.
[38] Y.Z. Li, B.L. Xu, Y.N. Fan, N. Feng, A.D. Qiu, J.W. Miao, J. He, H.P. Yang, Y. Chen, The effect of titania polymorph on the strong metal-support interaction of Pd/TiO_2 catalysts and their application in the liquid phase selective hydrogenation of long chain alkadienes, J. Mol. Catal. A: Chem. 216 (2004) 107–114.
[39] J. Yang, C.Q. Lv, Y. Guo, G.C. Wang, A DFT + U study of acetylene selective hydrogenation on oxygen defective anatase (101) and rutile (110) TiO_2 supported Pd_4 cluster, J. Chem. Phys. 136 (2012) 104107–104120.
[40] J.W. Wan, W.X. Chen, C.Y. Jia, L.R. Zheng, J.C. Dong, X.S. Zheng, Y. Wang, W.S. Yan, C. Chen, Q. Peng, D.S. Wang, Y.D. Li, Defect effects on TiO_2 nanosheets: stabilizing single atomic site Au and promoting catalytic properties, Adv. Mater. 30 (2018) 1705369–1705376.
[41] J. Yang, L.X. Cao, G.C. Wang, Acetylene hydrogenation on anatase TiO_2(101) supported Pd_4 cluster: oxygen deficiency effect, J. Mol. Model. 18 (2012) 3329–3339.
[42] H.Y. Liu, B.T. Teng, M.H. Fan, B.J. Wang, Y. Zhang, H. Gordon Harris, CH_4 dissociation on the perfect and defective MgO(001) supported Ni_4, Fuel 123 (2014) 285–292.
[43] J.K. Nørskov, T. Bligaard, J. Rossmeisl, C.H. Christensen, Towards the computational design of solid catalysts, Nat. Chem. 1 (2009) 37–46.
[44] B. Delley, An all-electron numerical method for solving the local density functional for polyatomic molecules, J. Chem. Phys. 92 (1990) 508–517.
[45] D.X. Tian, H.L. Zhang, J.J. Zhao, Structure and structural evolution of Ag_n(n = 3-22) clusters using a genetic algorithm and density functional theory method, Solid State Commun. 144 (2007) 174–179.
[46] J.P. Perdew, K. Burke, M. Ernzerhof, Generalized gradient approximation made simple, Phys. Rev. Lett. 77 (1996) 3865–3868.
[47] M. Dolg, U. Wedig, H. Stoll, H. Preuss, Energy-adjusted Ab initio pseudopotentials for the first row transition elements, J. Chem. Phys. 86 (1987) 866–872.
[48] Y. Inada, H. Orita, Efficiency of numerical basis sets for predicting the binding energies of hydrogen bonded complexes: evidence of small basis set superposition error compared to gaussian basis sets, J. Comput. Chem. 29 (2008) 225–232.
[49] T.A. Halgren, W.N. Lipscomb, The synchronous-transit method for determining reaction pathways and locating molecular rransition states, Chem. Phys. Lett. 49 (1977) 225–232.
[50] N. Govind, M. Petersen, G. Fitzgerald, D. King-Smith, J. Andzelm, A generalized synchronous transit method for transition state location, Comput. Mater. Sci. 28 (2003) 250–258.
[51] R.G. Zhang, B. Zhao, L.X. Ling, A.J. Wang, C.K. Russell, B.J. Wang, M.H. Fan, Cost-effective palladium-doped Cu bimetallic materials to tune selectivity and activity by using doped atom ensembles as active sites for efficient removal of acetylene from ethylene, Chem. Cat. Chem. 10 (2018) 2424–2432.
[52] B. Yang, R. Burch, C. Hardacre, G. Headdock, P. Hu, Influence of surface structures, subsurface carbon and hydrogen, and surface alloying on the activity and selectivity of acetylene hydrogenation on Pd surfaces: a density functional theory study, J. Catal. 305 (2013) 264–276.
[53] Y. Yang, J. Evans, J.A. Rodriguez, M.G. White, P. Liu, Fundamental studies of methanol synthesis from CO_2 hydrogenation on Cu(111), Cu clusters, and Cu/ZnO (0001), Phys. Chem. Chem. Phys. 12 (2010) 9909–9917.
[54] I.A. Hijazi, Y.H. Park, Structure of pure metallic nanoclusters: Monte Carlo simulation and Ab initio study, Eur. Phys. J. D. 59 (2010) 215–221.
[55] B. Zhao, R.G. Zhang, Z.X. Huang, B.J. Wang, Effect of the size of Cu clusters on selectivity and activity of acetylene selective hydrogenation, Appl. Catal. A: Gen. 546 (2017) 111–121.
[56] R.G. Zhang, M. Peng, T. Duan, B.J. Wang, Insight into size dependence of C_2 oxygenate synthesis from syngas on Cu cluster: the effect of cluster size on the selectivity, Appl. Surf. Sci. 407 (2017) 282–296.
[57] M.C. Valero, P. Raybaud, P. Sautet, Interplay between molecular adsorption and metal-support interaction for small supported metal clusters: CO and C_2H_4 adsorption on Pd_4/γ-Al_2O_3, J. Catal. 247 (2007) 339–355.
[58] L.D. Meng, G.C. Wang, A DFT + U study of acetylene selective hydrogenation over anatase supported Pd_aAg_b(a + b = 4) cluster, Phys. Chem. Chem. Phys. 16 (2014) 17541–17550.
[59] L. Xu, E.E. Stangland, M. Mavrikakis, Ethylene versus ethane: A DFT-based selectivity descriptor for efficient catalyst screening, J. Catal. 362 (2018) 18–24.
[60] J. Cheng, P. Hu, Theory of the kinetics of chemical potentials in heterogeneous catalysis, Angew. Chem. Int. Ed. 50 (2011) 7650–7654.
[61] J. Cheng, P. Hu, P. Ellis, S. French, G. Kelly, C.M. Lok, Brønsted-Evans-Polanyi relation of multistep reactions and volcano curve in heterogeneous catalysis, J. Phys. Chem. C 112 (2008) 1308–1311.
[62] X.M. Cao, R. Burch, C. Hardacre, P. Hu, An understanding of chemoselective hydrogenation on crotonaldehyde over Pt(111) in the free energy landscape: The microkinetics study based on first-principles calculations, Catal. Today 165 (2011) 71–79.
[63] K. Kontapakdee, J. Panpranot, P. Praserthdam, Effect of Ag addition on the properties of Pd-Ag/TiO_2 catalysts containing different TiO_2 crystalline phases, Catal. Commun. 8 (2007) 2166–2170.